

# General Synthetic Route to Double-Butterfly Fe/S Cluster Complexes via Reactions of the Dianions $\{[(\mu\text{-CO})\text{Fe}_2(\text{CO})_6]_2(\mu\text{-SZS-}\mu)\}^{2-}$ with Electrophiles<sup>†</sup>

Li-Cheng Song,\* Feng-Hua Gong, Tao Meng, Jian-Hua Ge, Li-Na Cui, and Qing-Mei Hu

Department of Chemistry, State Key Laboratory of Elemento-Organic Chemistry, Nankai University, Tianjin 300071, China

Received October 1, 2003

A simple and convenient route for the synthesis of linear and macrocyclic double-butterfly Fe/S cluster complexes has been developed, which involves a sequential reaction of  $\text{Fe}_3(\text{CO})_{12}$  with the dithiol HSZSH in the presence of  $\text{Et}_3\text{N}$ , followed by treatment of the intermediate  $[\text{Et}_3\text{NH}]^+$  salts of dianions  $\{[(\mu\text{-CO})\text{Fe}_2(\text{CO})_6]_2(\mu\text{-SZS-}\mu)\}^{2-}$  (**4**) with electrophiles. For example, treatment of the  $[\text{Et}_3\text{NH}]^+$  salts of dianions **4** with allyl bromide and  $\text{PhSBr}$  produces the linear complexes  $[(\mu\text{-CH}_2=\text{CHCH}_2)\text{Fe}_2(\text{CO})_6]_2(\mu\text{-SZS-}\mu)$  (**5a**,  $\text{Z} = (\text{CH}_2)_4$ ; **5b**,  $\text{Z} = \text{CH}_2(\text{CH}_2\text{OCH}_2)_2\text{CH}_2$ ; **5c**,  $\text{Z} = \text{CH}_2(\text{CH}_2\text{OCH}_2)_3\text{CH}_2$ ) and  $[(\mu\text{-PhS})\text{Fe}_2(\text{CO})_6]_2(\mu\text{-SZS-}\mu)$  (**6a**,  $\text{Z} = \text{CH}_2(\text{CH}_2\text{OCH}_2)_2\text{CH}_2$ ; **6b**,  $\text{Z} = \text{CH}_2(\text{CH}_2\text{OCH}_2)_3\text{CH}_2$ ), whereas treatment with  $\text{S}_2\text{Cl}_2$  and  $\text{ClSZSCl}$  yields the macrocyclic complexes  $[\text{Fe}_2(\text{CO})_6]_2(\mu\text{-S-S-}\mu)(\mu\text{-SZS-}\mu)$  (**7a**,  $\text{Z} = \text{CH}_2(\text{CH}_2\text{OCH}_2)_2\text{CH}_2$ ; **7b**,  $\text{Z} = \text{CH}_2(\text{CH}_2\text{OCH}_2)_3\text{CH}_2$ ) and  $[\text{Fe}_2(\text{CO})_6]_2(\mu\text{-SZS-}\mu)_2$  (**8a**,  $\text{Z} = \text{CH}_2(\text{CH}_2\text{OCH}_2)_2\text{CH}_2$ ; **8b**,  $\text{Z} = \text{CH}_2(\text{CH}_2\text{OCH}_2)_3\text{CH}_2$ ), respectively. In addition, while the  $[\text{Et}_3\text{NH}]^+$  salts of dianions **4** react in situ with  $\text{PhNCS}$  and  $\text{SCN}(\text{CH}_2)_4\text{NCS}$  to give the linear complexes  $[(\mu\text{-PhNHC=S})\text{Fe}_2(\text{CO})_6]_2(\mu\text{-SZS-}\mu)$  (**9a**,  $\text{Z} = \text{CH}_2\text{CH}_2\text{OCH}_2\text{CH}_2$ ; **9b**,  $\text{Z} = \text{CH}_2(\text{CH}_2\text{OCH}_2)_2\text{CH}_2$ ; **9c**,  $\text{Z} = \text{CH}_2(\text{CH}_2\text{OCH}_2)_3\text{CH}_2$ ) and macrocyclic complexes  $[\text{Fe}_2(\text{CO})_6]_2[\mu\text{-S=CNH}(\text{CH}_2)_4\text{NHC=S-}\mu](\mu\text{-SZS-}\mu)$  (**10a**,  $\text{Z} = (\text{CH}_2)_4$ ; **10b**,  $\text{Z} = \text{CH}_2(\text{CH}_2\text{OCH}_2)_2\text{CH}_2$ ), the in situ reactions with  $\text{PhC}\equiv\text{CPh}$  and  $\text{PhC}\equiv\text{CH}$  afford the linear complexes  $[(\mu\text{-}\sigma,\pi\text{-PhCH=CPh})\text{Fe}_2(\text{CO})_6]_2(\mu\text{-SZS-}\mu)$  (**11a**,  $\text{Z} = \text{CH}_2(\text{CH}_2\text{OCH}_2)_2\text{CH}_2$ ; **11b**,  $\text{Z} = \text{CH}_2(\text{CH}_2\text{OCH}_2)_3\text{CH}_2$ ) and  $[(\mu\text{-}\sigma,\pi\text{-PhCH=CH})\text{Fe}_2(\text{CO})_6]_2(\mu\text{-SZS-}\mu)$  (**12a**,  $\text{Z} = (\text{CH}_2)_4$ ; **12b**,  $\text{Z} = \text{CH}_2(\text{CH}_2\text{OCH}_2)_2\text{CH}_2$ ; **12c**,  $\text{Z} = \text{CH}_2(\text{CH}_2\text{OCH}_2)_3\text{CH}_2$ ). The possible pathways for production of these linear and macrocyclic cluster complexes are suggested, and their structures have been characterized by elemental analysis and IR and  $^1\text{H}$  NMR spectroscopy, as well as for **5a**, **7a**, **8a**, and **12a** by X-ray diffraction analysis.

## Introduction

Butterfly Fe/S cluster complexes have recently attracted growing interest, because of their novel chemistry<sup>1</sup> and the closely related biological relevance to the active site of the Fe-only hydrogenases.<sup>2</sup> Among them, the double-butterfly Fe/S cluster complexes<sup>3–11</sup> are of

particular interest. This is because that they might be expected, like double-tetrahedral  $\text{MoFeCoS}$  clusters,<sup>12</sup> to have new chemical reactivity patterns through the interactions between the two subcluster cores or, like double-cubane  $\text{MoFe}_3\text{S}_4$  clusters,<sup>13</sup> to become a new class of biologically relevant molecules. Previously, Seyferth's group and we reported a series of double-butterfly Fe/S cluster complexes, for instance **1–3**, which were prepared by reactions of  $(\mu\text{-S}_2)\text{Fe}_2(\text{CO})_6$  with alkyl lithium

\* To whom correspondence should be addressed. Fax: 0086-22-23504853. E-mail: lcsong@nankai.edu.cn.

<sup>†</sup> Dedicated to Professor Dietmar Seyferth, on the occasion of his 75th birthday and in recognition of his outstanding contributions to Organometallic Chemistry.

(1) For reviews, see for example: (a) Ogino, H.; Inomata, S.; Tobita, H. *Chem. Rev.* **1998**, *98*, 2093. (b) Song, L.-C. In *Advances in Organometallic Chemistry*; Huang, Y., Qian, Y., Eds.; Chemical Industry Press: Beijing, 1987; p 181. (c) Song, L.-C. In *Trends in Organometallic Chemistry*, Atwood, J. L., Corriu, R., Cowley, A. H., Lappert, M. F., Nakamura, A., Pereyre, M., Eds.; Research Trends: Trivandrum, India, 1999; Vol. 3, p 1.

(2) (a) Gloaguen, F.; Lawrence, J. D.; Rauchfuss, T. B. *J. Am. Chem. Soc.* **2001**, *123*, 9476. (b) Gloaguen, F.; Lawrence, J. D.; Schmidt, M.; Wilson, S. R.; Rauchfuss, T. B. *J. Am. Chem. Soc.* **2001**, *123*, 12518. (c) Lyon, E. J.; Georgakaki, I. P.; Reibenspies, J. H.; Darensbourg, M. Y. *J. Am. Chem. Soc.* **2001**, *123*, 3268. (d) Ott, S.; Kritikos, M.; Åkermark, B.; Sun, L. *Angew. Chem., Int. Ed.* **2003**, *42*, 3285. (e) Darensbourg, M. Y.; Lyon, E. J.; Zhao, X.; Georgakaki, I. P. *PNAS* **2003**, *100*, 3683. (f) Razavet, M.; Davies, S. C.; Hughes, D. L.; Barclay, J. E.; Evans, D. J.; Fairhurst, S. A.; Liu, X.; Pickett, C. J. *Dalton* **2003**, 586.

(3) Seyferth, D.; Kiwan, A. M.; Sinn, E. *J. Organomet. Chem.* **1985**, *281*, 111.

(4) Seyferth, D.; Kiwan, A. M. *J. Organomet. Chem.* **1985**, *286*, 219.

(5) Song, L.-C.; Kadiata, M.; Wang, J.-T.; Wang, R.-J.; Wang, H.-G. *J. Organomet. Chem.* **1988**, *340*, 239.

(6) Song, L.-C.; Kadiata, M.; Hu, Q.-M.; Wang, J.-T. *Acta Chim. Sin. (Engl. Ed.)* **1988**, 203.

(7) Song, L.-C.; Kadiata, M.; Wang, J.-T.; Wang, R.-J.; Wang, H.-G. *J. Organomet. Chem.* **1990**, *391*, 387.

(8) Song, L.-C.; Yan, C.-G.; Hu, Q.-M.; Wang, R.-J.; Mak, T. C. W. *Organometallics* **1995**, *14*, 5513.

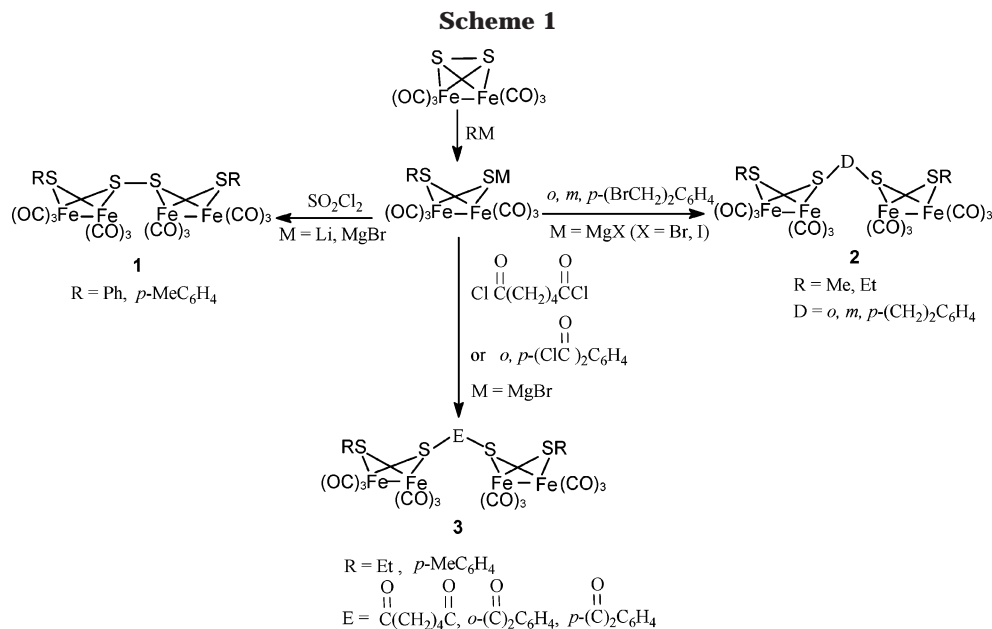
(9) Song, L.-C.; Yan, C.-G.; Hu, Q.-M.; Wang, R.-J.; Mak, T. C. W.; Huang, X.-Y. *Organometallics* **1996**, *15*, 1535.

(10) Song, L.-C.; Lu, G.-L.; Hu, Q.-M.; Yang, J.; Sun, J. *J. Organomet. Chem.* **2001**, *623*, 56.

(11) Bose, K. S.; Sinn, E.; Averill, B. A. *Organometallics* **1984**, *3*, 1126.

(12) Song, L.-C.; Guo, D.-S.; Hu, Q.-M.; Huang, X.-Y. *Organometallics* **2000**, *19*, 960.

(13) Kovacs, J. A.; Bashkin, J. K.; Holm, R. H. *J. Am. Chem. Soc.* **1985**, *107*, 1784.



or Grignard reagents and subsequent treatment of the S-centered monoanions  $(\mu\text{-RS})(\mu\text{-S}^-)\text{Fe}_2(\text{CO})_6$  with organic or inorganic halides (Scheme 1).<sup>4-7</sup>

Another synthetic route to double-butterfly Fe/S cluster complexes has also been developed. It involves the reactions of a new type of double-butterfly, two  $\mu\text{-CO}$ -containing dianions  $\{[(\mu\text{-CO})\text{Fe}_2(\text{CO})_6]_2(\mu\text{-SZS}\mu)\}^{2-}$  (**4**) with electrophiles, such as  $\text{Ph}_2\text{PCl}$  and  $\text{PhC}(\text{O})\text{Cl}$ .<sup>14</sup> To further develop the chemistry of novel dianions **4** and to see if this route has generality for the synthesis of double-butterfly Fe/S cluster compounds, we carried out the reactions of dianions **4** with other types of electrophiles, such as  $\text{CH}_2=\text{CHCH}_2\text{Br}$ ,  $\text{S}_2\text{Cl}_2$ ,  $\text{PhN}=\text{C}=\text{S}$ ,  $\text{PhC}\equiv\text{CH}$ ,  $\text{SCN}(\text{CH}_2)_2\text{NCS}$ , etc. As a result, a series of linear and cyclic double-butterfly Fe/S cluster complexes were produced. It follows that the route involving dianions **4** is indeed a general route suitable for synthesizing a wide variety of double-butterfly Fe/S cluster complexes. Now, we report the interesting results obtained from this study.

## Results and Discussion

**Synthesis and Characterization of  $[(\mu\text{-CH}_2=\text{CHCH}_2)\text{Fe}_2(\text{CO})_6]_2(\mu\text{-SZS}\mu)$  (**5a-c**).** The  $[\text{Et}_3\text{NH}]^+$  salts of dianions **4** ( $\text{Z} = (\text{CH}_2)_4$ ,  $\text{CH}_2(\text{CH}_2\text{OCH}_2)_{2,3}\text{CH}_2$ ) (generated from  $\text{Fe}_3(\text{CO})_{12}$ ,  $\text{HSZSH}$ , and  $\text{Et}_3\text{N}$ ) reacted in situ with an excess of allyl bromide in THF at room temperature (through nucleophilic attack of the two negatively charged Fe atoms of **4** at two molecules of allyl bromide followed by displacement of the two  $\mu\text{-CO}$  ligands in intermediate **m<sub>1</sub>**) to produce the series of double-butterfly cluster complexes **5a-c** (Scheme 2).

Products **5a-c** are red air-stable materials, whose elemental analysis and spectroscopic data are consistent with the structures shown in Scheme 2. The  $^1\text{H}$  NMR spectra of **5a-c** showed the  $\text{CH}_2$  proton signals of the allyl ligands as two doublets at ca. 0.5 ppm ( $J \approx 12$  Hz) and ca. 2 ppm ( $J \approx 6$  Hz), corresponding to the anti and syn hydrogens. An ORTEP drawing of **5a** is shown in Figure 1. Table 1 lists selected bond lengths and angles. Compound **5a** is a centrosymmetric double-butterfly cluster complex, in which two identical butterfly  $\text{Fe}_2\text{-SC}_3$  subcluster cores are joined together through its two

(14) (a) Song, L.-C.; Fan, H.-T.; Hu, Q.-M. *J. Am. Chem. Soc.* **2002**, *124*, 4566. (b) Song, L.-C.; Fan, H.-T.; Hu, Q.-M.; Yang, Z.-Y.; Sun, Y.; Gong, F.-H. *Chem. Eur. J.* **2003**, *9*, 170.

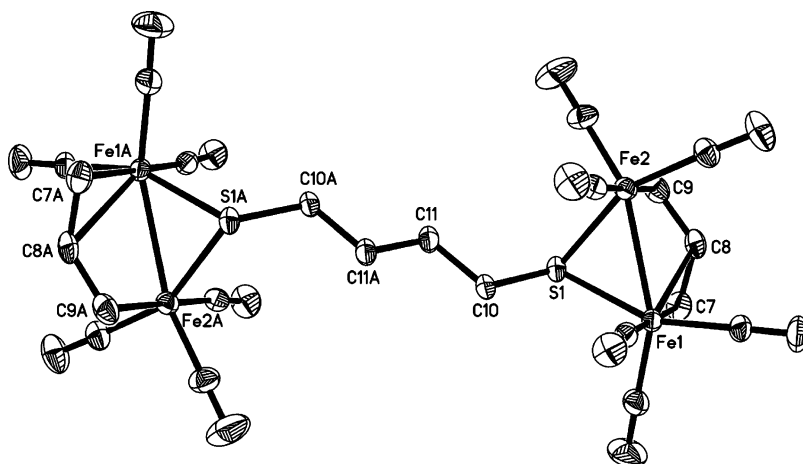


**Figure 1.** ORTEP drawing of **5a** with atom-labeling scheme.

**Table 1. Selected Bond Lengths (Å) and Angles (deg) for 5a**

Fe(1)–C(1)	1.771(5)	Fe(2)–C(9)	2.096(4)
Fe(1)–C(7)	2.110(4)	Fe(2)–S(1)	2.2181(13)
Fe(1)–S(1)	2.2232(14)	S(1)–C(10)	1.800(4)
Fe(1)–C(8)	2.429(4)	C(7)–C(8)	1.383(6)
Fe(1)–Fe(2)	2.6530(12)	C(8)–C(9)	1.403(6)
C(7)–Fe(1)–S(1)	86.96(13)	Fe(2)–S(1)–Fe(1)	73.36(5)
C(7)–Fe(1)–C(8)	34.56(14)	C(7)–C(8)–Fe(1)	60.0(2)
S(1)–Fe(1)–C(8)	82.24(11)	C(9)–C(8)–Fe(1)	114.0(3)
C(7)–Fe(1)–Fe(2)	89.34(13)	C(8)–C(9)–Fe(2)	89.7(3)
S(1)–Fe(1)–Fe(2)	53.23(3)	C(9)–Fe(2)–Fe(1)	85.92(13)
C(8)–Fe(1)–Fe(2)	59.16(11)	S(1)–Fe(2)–Fe(1)	53.41(4)

S atoms by a butylene group. The two S atoms attached to the butylene group are bound symmetrically across the two iron atoms (Fe(1)–S(1) = 2.2232(14) Å; Fe(2)–S(1) = 2.2181(13) Å), as are the two terminal carbon atoms in each of the allyl ligands (Fe(1)–C(7) = 2.110(4) Å; Fe(2)–C(9) = 2.096(4) Å). The C–C bond lengths of the allyl ligands (C(7)–C(8) = 1.383(6) Å; C(8)–C(9) = 1.403(6) Å) lie between the values reported for C–C single and double bonds, indicating that the ligands are best regarded as delocalized  $\pi$ -allyl ligands.<sup>15</sup> In addition, the dihedral angle between two wings of each butterfly subcluster core is 87.4° and the butylene bridge is connected to S atoms (the angle C(10)–S(1)–C(8) = 160.9°) by an equatorial type of bond.<sup>16</sup> In fact, the basic geometry of the subcluster cores in this double-butterfly cluster complex is very similar to that of the single-butterfly cluster complex ( $\mu$ -EtS)( $\mu$ -CH<sub>2</sub>=CHCH<sub>2</sub>)Fe<sub>2</sub>(CO)<sub>6</sub>.<sup>17</sup>

**Synthesis and Characterization of [( $\mu$ -PhS)Fe<sub>2</sub>(CO)<sub>6</sub>]<sub>2</sub>( $\mu$ -SZS- $\mu$ ) (**6a,b**), [Fe<sub>2</sub>(CO)<sub>6</sub>]<sub>2</sub>( $\mu$ -S–S- $\mu$ )( $\mu$ -SZS- $\mu$ ) (**7a,b**), and [Fe<sub>2</sub>(CO)<sub>6</sub>]<sub>2</sub>( $\mu$ -SZS- $\mu$ )<sub>2</sub> (**8a,b**).** While the [Et<sub>3</sub>NH]<sup>+</sup> salts of dianions **4** (Z = CH<sub>2</sub>(CH<sub>2</sub>OCH<sub>2</sub>)<sub>2,3</sub>CH<sub>2</sub>) reacted with PhSBr in THF at room temperature (through nucleophilic attack of the two negatively charged Fe atoms of **4** at two molecules of PhSBr and subsequent displacement of the two  $\mu$ -CO ligands in intermediate **m**<sub>2</sub>) to give the linear double-butterfly

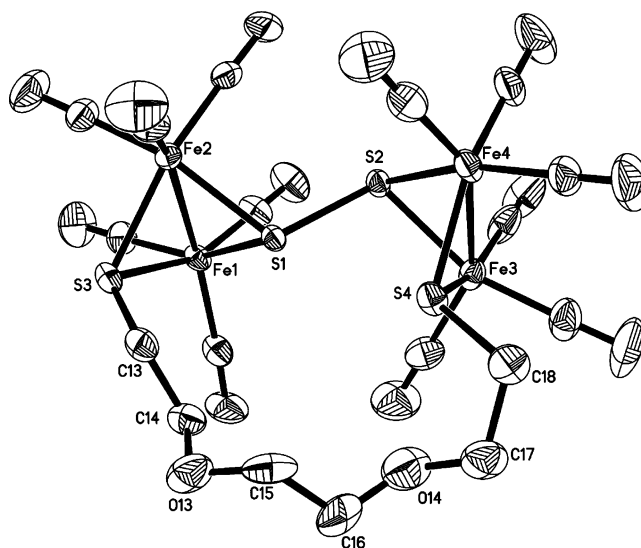


**Figure 2.** ORTEP drawing of **7a** with atom-labeling scheme.

complexes **6a,b**, they reacted with S<sub>2</sub>Cl<sub>2</sub> and ClSZSCl (Z = CH<sub>2</sub>(CH<sub>2</sub>OCH<sub>2</sub>)<sub>2,3</sub>CH<sub>2</sub>) under similar conditions (through double nucleophilic attack of the two negatively charged Fe atoms of **4** at one molecule of S<sub>2</sub>Cl<sub>2</sub> or ClSZSCl followed by loss of two  $\mu$ -CO ligands from intermediate **m**<sub>3</sub> or **m**<sub>4</sub>) to afford the macrocyclic cluster complexes **7a,b** and **8a,b**, respectively (Scheme 3).

Products **6a,b**, **7a,b**, and **8a,b** may be regarded as new types of acyclic and cyclic cluster crown ethers, which have been characterized by elemental analyses and IR and <sup>1</sup>H NMR spectroscopy, as well as for **7a** and **8a** by X-ray diffraction analyses. While the <sup>1</sup>H NMR spectra of **6a,b**, **7a,b**, and **8a,b** displayed the corresponding H-containing organic groups, their IR spectra exhibited several absorption bands in the range 2081–1966 cm<sup>-1</sup> for their terminal carbonyls and one absorption band in the region 1128–1116 cm<sup>-1</sup> for their ether chain functionalities.

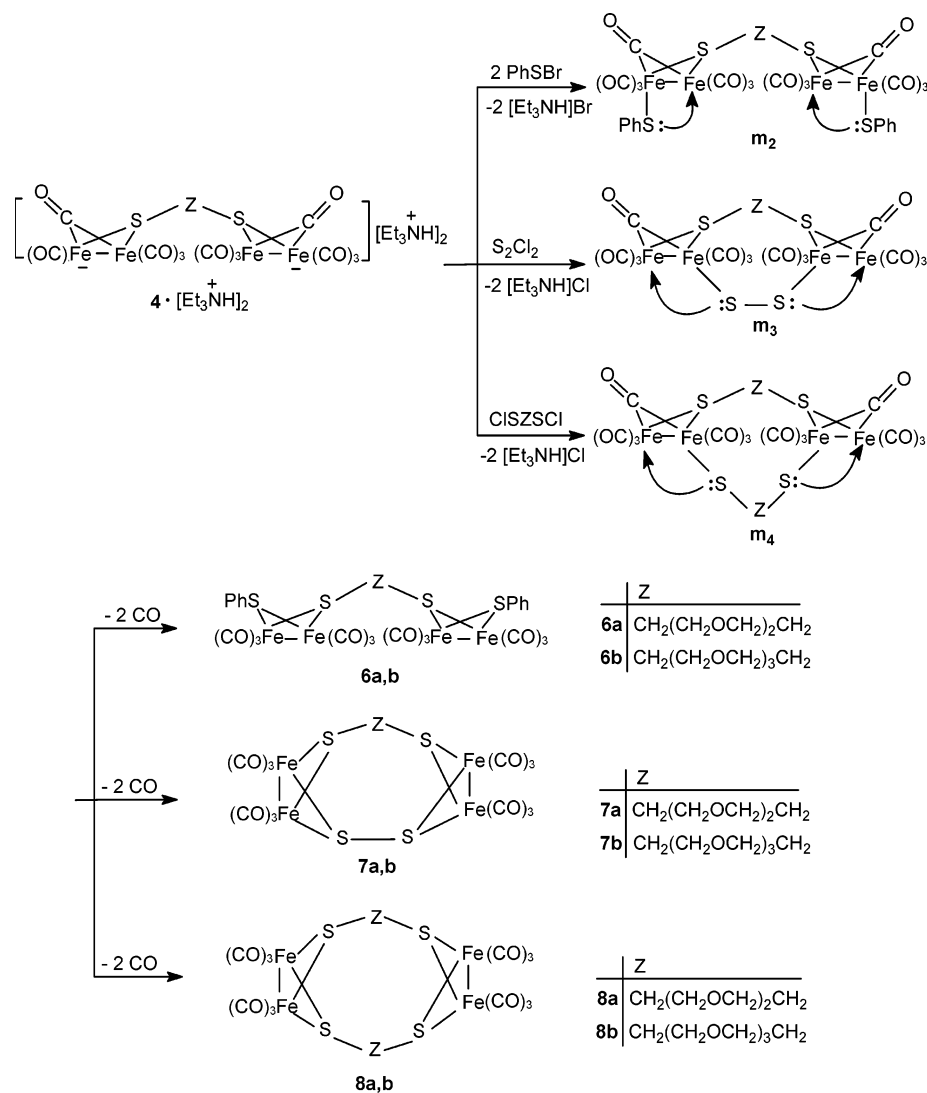
Figure 2 shows the molecular structure of **7a**, and Table 2 displays its bond lengths and angles. As can be seen in Figure 2, complex **7a** contains the two butterfly subcluster cores Fe(1)Fe(2)S(1)S(3) and Fe(3)Fe(4)S(2)S(4), which are connected by a S(1)–S(2) bond and the ether chain C(13)C(14)O(13)C(15)C(16)O(14)C(17)C(18) to afford a 16-membered macrocycle.

(15) MacGillavry, C. H.; Rieck, G. D., Eds. *International Tables for X-ray Crystallography*; Kynoch Press: Birmingham, England, 1974; Vol. III, p 276.

(16) (a) Seyferth, D.; Henderson, R. S.; Song, L.-C. *Organometallics* **1982**, *1*, 125. (b) Shaver, A.; Fitzpatrick, P. J.; Steliou, K.; Butler, I. S. *J. Am. Chem. Soc.* **1979**, *101*, 1313.

(17) Seyferth, D.; Womack, G. B.; Dewan, J. C. *Organometallics* **1985**, *4*, 398.

Scheme 3

Table 2. Selected Bond Lengths (Å) and Angles (deg) for **7a**

Fe(1)–C(1)	1.808(6)	Fe(1)–S(3)	2.286(2)
Fe(1)–C(2)	1.800(7)	Fe(2)–S(3)	2.2802(18)
Fe(1)–S(1)	2.239(2)	Fe(3)–S(4)	2.2581(19)
Fe(2)–S(1)	2.2428(18)	Fe(3)–Fe(4)	2.5304(17)
Fe(1)–Fe(2)	2.5103(16)	S(1)–S(2)	2.118(2)
S(1)–Fe(1)–S(3)	78.30(5)	S(1)–Fe(2)–S(3)	78.34(7)
S(1)–Fe(1)–Fe(2)	56.01(4)	S(1)–Fe(2)–Fe(1)	55.87(6)
S(3)–Fe(1)–Fe(2)	56.55(4)	S(2)–Fe(3)–S(4)	80.89(6)
S(4)–Fe(4)–S(2)	80.86(5)	S(2)–Fe(3)–Fe(4)	55.96(6)
S(4)–Fe(4)–Fe(3)	55.95(5)	Fe(1)–S(1)–Fe(2)	68.12(5)
S(2)–S(1)–Fe(1)	111.78(7)	S(2)–S(1)–Fe(2)	113.78(7)

In addition, the ether chain is bound to S(3) by the axial bond C(13)–S(3) (the angle C(13)–S(3)⋯S(1) = 77.9°) and to S(4) by the equatorial bond C(18)–S(4) (the angle C(18)–S(4)⋯S(2) = 158.0°), whereas the subcluster core Fe(1)Fe(2)S(1)S(3) is bonded to S(2) by its equatorial bond (the angle S(2)–S(1)⋯S(3) = 159.1°) and the subcluster core Fe(3)Fe(4)S(2)S(4) to S(1) by its axial bond (the angle S(1)–S(2)⋯S(4) = 74.4°),<sup>16</sup> respectively. The S–S bond (2.118(2) Å) of **7a** is lengthened from the single S–S bond (2.037(5) Å) in elemental sulfur.<sup>18</sup> It is

Table 3. Selected Bond Lengths (Å) and Angles (deg) for **8a**

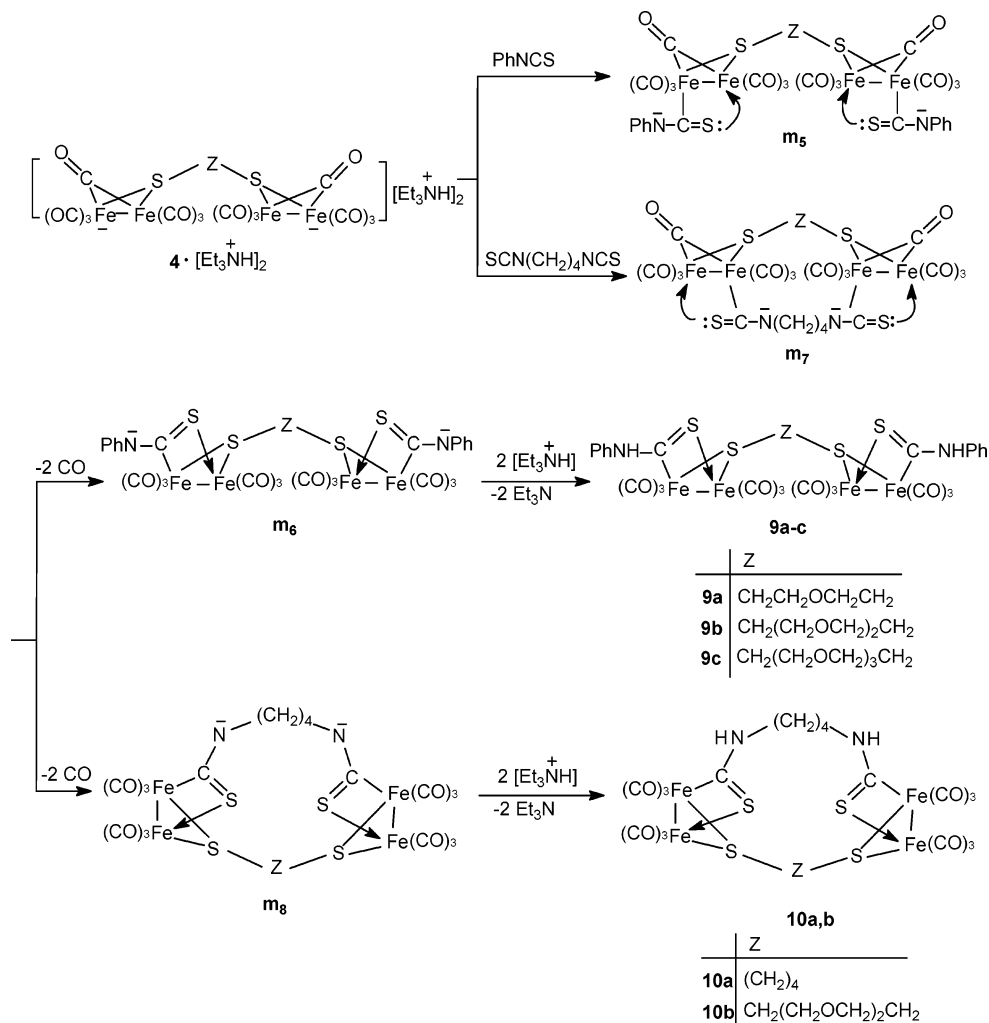
Fe(1)–C(1)	1.793(7)	Fe(2)–S(2A)	2.2592(19)
Fe(1)–S(1)	2.2468(19)	S(1)–C(7)	1.838(6)
Fe(2)–S(1)	2.2541(19)	S(2)–C(12)	1.842(6)
Fe(1)–S(2A)	2.2601(18)	Fe(2)–C(4)	1.788(7)
Fe(1)–Fe(2)	2.5130(14)	S(2)–Fe(1A)	2.2601(18)
C(1)–Fe(1)–S(1)	94.1(2)	S(1)–Fe(2)–S(2A)	80.32(7)
S(1)–Fe(1)–S(2A)	80.46(6)	S(1)–Fe(2)–Fe(1)	55.92(5)
C(1)–Fe(1)–Fe(2)	102.8(2)	S(2A)–Fe(2)–Fe(1)	56.23(5)
S(1)–Fe(1)–Fe(2)	56.20(5)	C(7)–S(1)–Fe(1)	114.6(2)
S(2A)–Fe(1)–Fe(2)	56.20(5)	Fe(1)–S(1)–Fe(2)	67.88(6)

also lengthened compared to the S–S bond (2.108(3) Å) of the linear double cluster complex  $[(\mu\text{-PhS})\text{Fe}_2(\text{CO})_6]_2$  ( $\mu\text{-S-S-}\mu$ ),<sup>3</sup> obviously due to formation of its 16-membered ring, in which the ether chain pulls the two butterfly  $\text{Fe}_2\text{S}_2$  cluster cores closer and thus makes the S–S bond longer.

The molecular structure of **8a** is shown in Figure 3, and its bond lengths and angles are displayed in Table 3. Similar to **7a**, product **8a** is composed of the two butterfly cluster cores Fe(1)Fe(2)S(1)S(2A) and Fe(1A)Fe(2A)S(2)S(1A) linked together by the two ether chains C(7)C(8)O(7)C(9)C(10)O(8)C(11)C(12) and C(7A)C(8A)O(7A)C(9A)C(10A)O(8A)C(11A)C(12A) to form a 24-membered macrocycle. The heteroatom distances

(18) Anderson, E. L.; Fehlner, T. P.; Foti, A. E.; Salahub, D. R. *J. Am. Chem. Soc.* **1980**, *102*, 7422.

Scheme 4



S(1)–S(1A), S(2)–S(2A), O(7)–O(7A), and O(8)–O(8A) are in the range 7.122–8.815 Å. While one ether chain is bonded to S(1) and S(2) by the equatorial bond C(7)–S(1) (the angle C(7)–S(1)⋯S(2A) = 158.8°) and axial bond C(12)–S(2) (the angle C(12)–S(2)⋯S(1A) = 79.8°), the other ether chain is bound to S(1A) and S(2A) by the equatorial bond C(7A)–S(1A) (the angle C(7A)–S(1A)⋯S(2) = 158.5°) and axial bond C(12A)–S(2A) (the angle C(12A)–S(2A)⋯S(1) = 79.8°),<sup>16</sup> respectively. However, in contrast to **7a**, product **8a** has two identical ether chains, whose structure is centrosymmetric. To our knowledge, both **7a** and **8a** are so far the first crystallographically characterized cyclic double-butterfly Fe<sub>2</sub>S<sub>2</sub> clusters.

**Synthesis and Characterization of  $[(\mu\text{-PhNHC}=\text{S})\text{Fe}_2(\text{CO})_6]_2(\mu\text{-SZS}-\mu)$  (**9a-c**),  $[\text{Fe}_2(\text{CO})_6]_2(\mu\text{-S}=\text{CNH}(\text{CH}_2)_4\text{NHC}=\text{S}-\mu)(\mu\text{-SZS}-\mu)$  (**10a,b**),  $[(\mu\text{-}\sigma,\pi\text{-PhCH}=\text{CPh})\text{Fe}_2(\text{CO})_6]_2(\mu\text{-SZS}-\mu)$  (**11a,b**), and  $[(\mu\text{-}\sigma,\pi\text{-PhCH}=\text{CH})\text{Fe}_2(\text{CO})_6]_2(\mu\text{-SZS}-\mu)$  (**12a-c**).** We further found that the  $[\text{Et}_3\text{NH}]^+$  salts of dianions **4** not only reacted with the electrophiles having one and two leaving groups to produce the linear and cyclic double-butterfly clusters of types **5–8** as described above, but also they could react with the electrophiles that have no leaving group to yield the corresponding linear and cyclic double-butterfly clusters. For example, the  $[\text{Et}_3\text{NH}]^+$  salts of **4** (Z =  $\text{CH}_2(\text{CH}_2\text{OCH}_2)_{1-3}\text{CH}_2$ ) reacted with phenyl isothiocyanate in THF at room temperature to

afford the double-butterfly cluster compounds **9a-c**, whereas the  $[\text{Et}_3\text{NH}]^+$  salts of dianions **4** (Z =  $(\text{CH}_2)_4$ ,  $\text{CH}_2(\text{CH}_2\text{OCH}_2)_2\text{CH}_2$ ) reacted with diisothiocyanate  $\text{SCN}(\text{CH}_2)_4\text{NCS}$  under similar conditions to yield the macrocyclic double-butterfly clusters **10a,b** (Scheme 4). Clusters **9a-c** might be suggested as being derived from nucleophilic attack of the two negatively charged Fe atoms of **4** at the central C atoms of two molecules of PhNCS followed by loss of two  $\mu\text{-CO}$  ligands of dianions **m<sub>5</sub>** and protonation of the N-centered dianions **m<sub>6</sub>** by

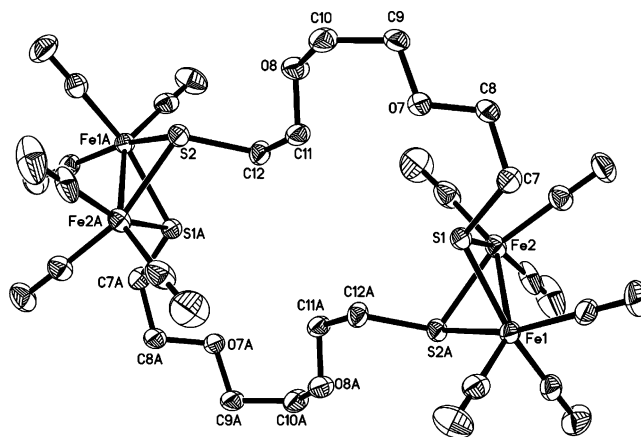
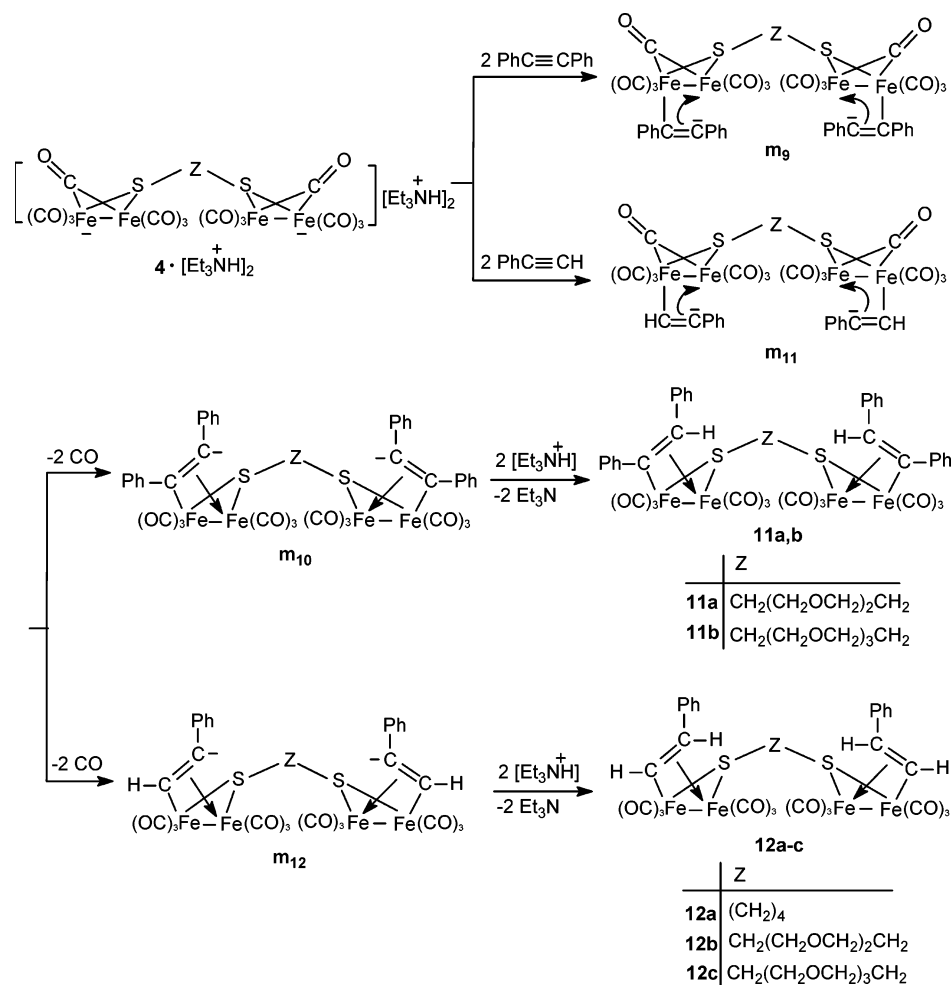


**Figure 3.** ORTEP drawing of **8a** with atom-labeling scheme.

Scheme 5



the counterion  $[\text{Et}_3\text{NH}]^+$ ; similarly, clusters **10a,b** could be regarded as produced through nucleophilic attack of the two negatively charged Fe atoms of **4** at the central C atoms in two  $\text{N}=\text{C}=\text{S}$  functional groups of one molecule of the diisothiocyanate followed by loss of two  $\mu\text{-CO}$  ligands from dianions **m<sub>7</sub>** and protonation of the N-centered dianions **m<sub>8</sub>** by the  $[\text{Et}_3\text{NH}]^+$  cation (Scheme 4).

Clusters **9a–c** and **10a,b** have been characterized by elemental analysis and spectroscopy. For example, while their  $^1\text{H}$  NMR spectra showed one singlet at about 9 ppm for **9a–c** and about 7 ppm for **10a,b** assigned to their NH groups, their IR spectra displayed one absorption band in the range  $940\text{--}1026\text{ cm}^{-1}$  for their coordinated thiocarbonyl  $\text{C}=\text{S}$  groups.<sup>19</sup> In fact, the formation of  $\text{PhNHC}=\text{S}$  and  $\text{S}=\text{CHN}(\text{CH}_2)_4\text{NHC}=\text{S}$  ligands in the above-mentioned reactions could be strongly supported by the crystal structure of the single-butterfly cluster ( $\mu\text{-}p\text{-MeC}_6\text{H}_4\text{Se})(\mu\text{-PhCH}_2\text{NHC}=\text{S})\text{Fe}_2(\text{CO})_6$ , produced from reaction of the  $[\text{Et}_3\text{NH}]^+$  salt of the monoanion  $[(\mu\text{-}p\text{-MeC}_6\text{H}_4\text{Se})(\mu\text{-CO})\text{Fe}_2(\text{CO})_6]^-$  with  $\text{PhCH}_2\text{NCS}$ .<sup>20</sup>

Similarly, the  $[\text{Et}_3\text{NH}]^+$  salts of dianions **4** ( $\text{Z} = (\text{CH}_2)_4, \text{CH}_2(\text{CH}_2\text{OCH}_2)_{2,3}\text{CH}_2$ ) reacted with diphenyl-

acetylene and phenylacetylene in refluxing THF to give the double-butterfly cluster complexes **11a,b** and **12a–c**, respectively (Scheme 5).

Apparently, **11a,b** were presumably formed by nucleophilic attack of the two negatively charged Fe atoms in **4** at the triply bonded C atoms of two molecules of diphenylacetylene, followed by loss of two  $\mu\text{-CO}$  ligands from the C-centered dianions **m<sub>9</sub>** and protonation of another C-centered dianion **m<sub>10</sub>** by the  $[\text{Et}_3\text{NH}]^+$  cation; similarly, **12a–c** might be produced by protonation of the C-centered dianions **m<sub>12</sub>** by the  $[\text{Et}_3\text{NH}]^+$  cation, which were formed by nucleophilic attack of the two negatively charged Fe atoms of **4** at  $\beta\text{-C}$  atoms of two phenylacetylene molecules (both steric considerations and the ability of the phenyl group to stabilize  $\alpha\text{-carbanions}$  favor  $\beta\text{-attack}$  of the iron nucleophile), followed by loss of two  $\mu\text{-CO}$  ligands from the initially formed C-centered dianions **m<sub>11</sub>** (Scheme 5).

In the  $^1\text{H}$  NMR spectra of complexes **11a,b** and **12a–c**, the *endo*-PhCH signals for **11a,b** are overlapped with their  $\text{CH}_2\text{O}$  signals as a multiplet from 3.6 to 3.7 ppm, whereas the *endo*-PhCH signals for **12a–c** are found as an upfield doublet ( $\delta_{\text{H}} \sim 4.3\text{ ppm}$ ,  $J_{\text{trans}} \approx 13\text{ Hz}$ ) and the *endo*-FeCH signals for **12a–c** appear as a low-field doublet ( $\delta_{\text{H}} \sim 8.4\text{ ppm}$ ,  $J_{\text{trans}} \approx 13\text{ Hz}$ ). These data agree with the corresponding data reported by Seyferth and King for the single-butterfly complexes ( $\mu\text{-}\sigma,\pi\text{-PhCH}=\text{CH})(\mu\text{-}^t\text{BuS})\text{Fe}_2(\text{CO})_6$ ,<sup>21</sup> ( $\mu\text{-}\sigma,\pi\text{-PhCH}=\text{CPh})(\mu\text{-}^t\text{BuS})\text{Fe}_2\text{-}$

(19) (a) Patin, H.; Magnani, G.; Mahé, C.; Le Marouille, J.-Y.; Southern, T. G.; Benoit, A.; Grandjean, D. *J. Organomet. Chem.* **1980**, *197*, 315. (b) Song, L.-C.; Yan, C.-G.; Hu, Q.-M.; Wu, B.-M.; Mak, T. C. W. *Organometallics* **1997**, *16*, 632.

(20) Song, L.-C.; Lu, G.-L.; Hu, Q.-M.; Fan, H.-T.; Chen, J.; Sun, J.; Huang, X.-Y. *J. Organomet. Chem.* **2001**, *627*, 255.

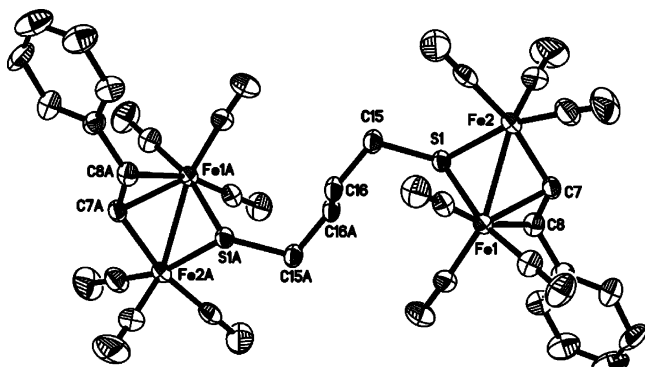


**Figure 4.** ORTEP drawing of **12a** with atom-labeling scheme.

**Table 4.** Selected Bond Lengths (Å) and Angles (deg) for **12a**

Fe(1)–C(8)	2.235(6)	Fe(3)–Fe(4)	2.5517(13)
Fe(1)–S(1)	2.2737(17)	Fe(4)–S(2)	2.2563(17)
Fe(1)–Fe(2)	2.5395(14)	S(1)–C(15)	1.824(5)
Fe(2)–C(7)	1.974(6)	C(7)–C(8)	1.393(8)
Fe(3)–S(2)	2.2751(17)	C(8)–C(9)	1.502(8)
S(1)–Fe(1)–Fe(2)	55.43(5)	S(2)–Fe(4)–Fe(3)	56.08(5)
S(1)–Fe(2)–Fe(1)	56.28(5)	Fe(2)–S(1)–Fe(1)	68.28(5)
C(7)–C(8)–C(9)	126.2(6)	Fe(4)–S(2)–Fe(3)	68.54(5)
C(7)–C(8)–Fe(1)	65.5(3)	C(8)–C(7)–Fe(2)	127.9(4)
C(9)–C(8)–Fe(1)	121.3(4)	C(8)–C(7)–Fe(1)	77.1(3)
S(2)–Fe(3)–Fe(4)	55.38(5)	Fe(2)–C(7)–Fe(1)	77.4(2)

(CO)<sub>6</sub>,<sup>21</sup> and (*μ*-σ,π-CH=CH)(*μ*-RS)Fe<sub>2</sub>(CO)<sub>6</sub>.<sup>22</sup> Thus, from the <sup>1</sup>H NMR data for the vinyl ligand in double-cluster complexes **11a,b** and **12a–c**, it was determined that overall addition of the diiron unit and the proton to the two molecules of acetylenes occurred in a cis fashion. This is completely consistent with the addition mode between the [Et<sub>3</sub>NH]<sup>+</sup> salts of single-butterfly anions [(*μ*-RS)(*μ*-CO)Fe<sub>2</sub>(CO)<sub>6</sub>]<sup>−</sup> and acetylenes to form the corresponding single-butterfly complexes (*μ*-σ,π-R<sup>1</sup>-CH=CR<sup>2</sup>)(*μ*-RS)Fe<sub>2</sub>(CO)<sub>6</sub>.<sup>21</sup>

The molecular structure of **12a** is shown in Figure 4, while selected bond lengths and angles are presented in Table 4. Complex **12a**, similar to **5a**, is also a centrosymmetric double-butterfly cluster complex, which contains two butterfly Fe<sub>2</sub>SC<sub>2</sub> subcluster cores coupled together by a butylene group. However, in contrast to **5a**, the two S atoms attached to the butylene group and the two C atoms of substituted vinyl ligands in **12a** are asymmetrically bonded to the two iron atoms (Fe(1)–S(1) = 2.2737(17) Å; Fe(2)–S(1) = 2.2509(17) Å; Fe(1)–C(8) = 2.235(6) Å; Fe(2)–C(7) = 1.974(6) Å). It is noteworthy that the C–C bond length of the substituted vinyl ligand (C(7)–C(8) = 1.393(8) Å) is obviously longer than the normal value for a C–C double bond, which demonstrates that the C–C double bond in each of the substituted vinyl ligands is coordinated to the two iron atoms in a σ,π-manner (Fe(2)–C(7) σ-bond length 1.974(6) Å; Fe(1)–C(7) and Fe(1)–C(8) π-bond lengths 2.087(6) and 2.235(6) Å, respectively). Finally, it is also worth noting that the dihedral angle between the two butterfly wings Fe(2)–Fe(1)–S(1) and Fe(1)–Fe(2)–C(7)–C(8) (109.5°) is much larger than the correspond-

ing angle in **5a** (87.4°) and the subcluster cores are also linked through S atoms by an equatorial type of bond<sup>16</sup> (the angle C(15)–S(1)⋯C(7) = C(15A)–S(1A)⋯C(7A) = 151.4°).

## Experimental Section

**General Comments.** All reactions were carried out under an atmosphere of prepurified nitrogen by using standard Schlenk and vacuum-line techniques. Tetrahydrofuran (THF) was distilled from Na/benzophenone ketyl under nitrogen and bubbled for ca. 30 min before use. Fe<sub>3</sub>(CO)<sub>12</sub>,<sup>23</sup> HSZSH (Z = (CH<sub>2</sub>)<sub>4</sub>, CH<sub>2</sub>(CH<sub>2</sub>OCH<sub>2</sub>)<sub>n</sub>CH<sub>2</sub> (n = 1–3)),<sup>24</sup> PhSBr,<sup>25</sup> ClSZSCl (Z = CH<sub>2</sub>(CH<sub>2</sub>OCH<sub>2</sub>)<sub>n</sub>CH<sub>2</sub> (n = 2, 3)),<sup>26</sup> SCN(CH<sub>2</sub>)<sub>4</sub>NCS,<sup>27</sup> and PhC≡CH<sup>28</sup> were prepared according to literature procedures. CH<sub>2</sub>=CHCH<sub>2</sub>Br, S<sub>2</sub>Cl<sub>2</sub>, and PhNCS were of commercial origin and used without further purification. Preparative TLC was carried out on glass plates (25 × 15 × 0.25) coated with silica gel G (10–40 μm). IR spectra were recorded on a Bio-Rad FTS 135 infrared spectrophotometer. <sup>1</sup>H NMR spectra were taken on a Bruker AC-P200 NMR spectrometer. C/H analyses were performed with an Elementar Vario EL analyzer. Melting points were determined on a Yanaco MP-500 apparatus and were uncorrected.

**Standard in Situ Preparation of the [Et<sub>3</sub>NH]<sup>+</sup> Salts of Dianions** {[(*μ*-CO)Fe<sub>2</sub>(CO)<sub>6</sub>]<sub>2</sub>(*μ*-SZS-*μ*)}<sup>2−</sup> (**4**·[Et<sub>3</sub>NH]<sub>2</sub>). A 100 mL three-necked flask fitted with a magnetic stir bar, a rubber septum, and a nitrogen inlet tube was charged with 1.00 g (2.0 mmol) of Fe<sub>3</sub>(CO)<sub>12</sub>, 30 mL of THF, 1.0 mmol of HSZSH (Z = (CH<sub>2</sub>)<sub>4</sub>, CH<sub>2</sub>(CH<sub>2</sub>OCH<sub>2</sub>)<sub>n</sub>CH<sub>2</sub> (n = 1–3)) and 0.28 mL (2.0 mmol) of Et<sub>3</sub>N. The mixture was stirred at room temperature for 45 min to give a brown-red solution of ca. 1 mmol of the intermediate salts **4**·[Et<sub>3</sub>NH]<sub>2</sub>, which was utilized immediately in the following preparations.

**Preparation of [(*μ*-CH<sub>2</sub>=CHCH<sub>2</sub>)Fe<sub>2</sub>(CO)<sub>6</sub>]<sub>2</sub>[*μ*-S(CH<sub>2</sub>)<sub>4</sub>S-*μ*] (**5a**).** To the above-prepared solution of **4**·[Et<sub>3</sub>NH]<sub>2</sub> (Z = (CH<sub>2</sub>)<sub>4</sub>) was added 0.70 mL (8.0 mmol) of CH<sub>2</sub>=CHCH<sub>2</sub>Br, and the mixture was stirred at room temperature for 16 h. The solvent was removed under reduced pressure. The residue was subjected to TLC separation using CH<sub>2</sub>Cl<sub>2</sub>/petroleum ether (1/4 v/v) as eluent. From the main red band, 0.190 g (25%) of **5a** was obtained as a red solid, mp 125 °C dec. Anal. Calcd for C<sub>22</sub>H<sub>18</sub>Fe<sub>4</sub>O<sub>12</sub>S<sub>2</sub>: C, 34.68; H, 2.38. Found: C, 34.45; H, 2.28. IR (KBr disk): ν<sub>C=O</sub> 2059 (vs), 2025 (vs), 1965 (vs) cm<sup>−1</sup>. <sup>1</sup>H NMR (200 MHz, CDCl<sub>3</sub>): 0.48 (d, J = 11.9 Hz, 4H, 4 anti-FeCHH), 1.69 (s, 4H, CH<sub>2</sub>CH<sub>2</sub>CH<sub>2</sub>CH<sub>2</sub>), 1.98 (d, J = 5.6 Hz, 4H, 4 syn-FeCHH), 2.44 (s, 4H, 2CH<sub>2</sub>S), 4.70–4.85 (m, 2H, 2 allylic CH) ppm.

**Preparation of [(*μ*-CH<sub>2</sub>=CHCH<sub>2</sub>)Fe<sub>2</sub>(CO)<sub>6</sub>]<sub>2</sub>[*μ*-SCH<sub>2</sub>-(CH<sub>2</sub>OCH<sub>2</sub>)<sub>2</sub>CH<sub>2</sub>S-*μ*] (**5b**).** The same procedure was followed as for **5a**, but **4**·[Et<sub>3</sub>NH]<sub>2</sub> (Z = CH<sub>2</sub>(CH<sub>2</sub>OCH<sub>2</sub>)<sub>2</sub>CH<sub>2</sub>) was used. From the main red band, 0.259 g (32%) of **5b** was obtained as a red oil. Anal. Calcd for C<sub>24</sub>H<sub>22</sub>Fe<sub>4</sub>O<sub>14</sub>S<sub>2</sub>: C, 35.07; H, 2.70. Found: C, 34.48; H, 2.96. IR (KBr disk): ν<sub>C=O</sub> 2061 (s), 2020 (vs), 1950 (vs); ν<sub>C–O–C</sub> 1110 (m) cm<sup>−1</sup>. <sup>1</sup>H NMR (200 MHz, CDCl<sub>3</sub>): 0.51 (d, J = 10.2 Hz, 4H, 4 anti-FeCHH), 1.97 (d, J = 6.1 Hz, 4H, 4 syn-FeCHH), 2.65 (s, 4H, 2CH<sub>2</sub>S), 3.62 (s, 8H, 4CH<sub>2</sub>O), 4.60–5.05 (m, 2H, 2 allylic CH) ppm.

**Preparation of [(*μ*-CH<sub>2</sub>=CHCH<sub>2</sub>)Fe<sub>2</sub>(CO)<sub>6</sub>]<sub>2</sub>[*μ*-SCH<sub>2</sub>-(CH<sub>2</sub>OCH<sub>2</sub>)<sub>3</sub>CH<sub>2</sub>S-*μ*] (**5c**).** The same procedure was followed as for **5a**, but **4**·[Et<sub>3</sub>NH]<sub>2</sub> (Z = CH<sub>2</sub>(CH<sub>2</sub>OCH<sub>2</sub>)<sub>3</sub>CH<sub>2</sub>) was utilized. From the main red band, 0.208 g (24%) of **5c** was

(23) King, R. B. *Organometallic Syntheses, Transition-Metal Compounds*; Academic Press: New York, 1965; Vol. I, p 95.

(24) (a) Martin, D. J.; Greco, C. C. *J. Org. Chem.* **1968**, *33*, 1275. (b) Pedersen, C. J. *J. Am. Chem. Soc.* **1967**, *89*, 7017.

(25) Harpp, D. N.; Mathiaparanam, P. *J. Org. Chem.* **1972**, *37*, 1367.

(26) Morris, J. L.; Rees, C. W.; *J. Chem. Soc., Perkin Trans. 1* **1987**, 211.

(27) Martha, W., Ed. *The Merck Index*, 11th ed.; Merck: Rahway, NJ, 1988; p 293.

(28) Hessler, J. C. *Organic Syntheses*; Wiley: New York, 1955; Collect. Vol. 3, p 438.

(21) Seyferth, D.; Hoke, J. B.; Womack, G. B. *Organometallics* **1990**, *9*, 2662.

(22) King, R. B.; Treichel, P. M.; Stone, F. G. A. *J. Am. Chem. Soc.* **1961**, *83*, 3600.

obtained as a red oil. Anal. Calcd for  $C_{26}H_{26}Fe_4O_{15}S_2$ : C, 36.06; H, 3.02. Found: C, 36.00; H, 2.95. IR (KBr disk):  $\nu_{C=O}$  2061 (s), 2016 (vs), 1955 (vs);  $\nu_{C-O-C}$  1108 (m)  $cm^{-1}$ .  $^1H$  NMR (200 MHz,  $CDCl_3$ ): 0.49 (d,  $J = 12.5$  Hz, 4H, 4 anti- $FeCHH$ ), 1.98 (d,  $J = 5.6$  Hz, 4H, 4 syn- $FeCHH$ ), 2.62–2.67 (m, 4H,  $2CH_2S$ ), 3.63 (s, 12H,  $6CH_2O$ ), 4.70–4.85 (m, 2H, 2 allylic CH) ppm.

**Preparation of  $[(\mu-PhS)Fe_2(CO)_6]_2[\mu-SCH_2(CH_2OCH_2)_2-CH_2S-\mu]$  (6a).** To the above-prepared solution of  $4 \cdot [Et_3NH]_2$  ( $Z = CH_2(CH_2OCH_2)_2CH_2$ ) was added 0.378 g (2.0 mmol) of PhSBr, and the mixture was stirred at room temperature for 12 h. Solvent was removed under reduced pressure. The residue was subjected to TLC separation using  $CH_2Cl_2$ /petroleum ether (1/1 v/v) as eluent. From the main red band, 0.342 g (36%) of **6a** was obtained as a red solid, mp 146 °C dec. Anal. Calcd for  $C_{30}H_{22}Fe_4O_{14}S_4$ : C, 37.61; H, 2.31. Found: C, 37.53; H, 2.25. IR (KBr disk):  $\nu_{C=O}$  2070 (s), 2032 (vs), 1990 (vs), 1968 (vs);  $\nu_{C-O-C}$  1125 (s)  $cm^{-1}$ .  $^1H$  NMR (200 MHz,  $CDCl_3$ ): 2.52 (t,  $J = 6.4$  Hz, 4H,  $2CH_2S$ ), 3.50–3.62 (m, 8H,  $4CH_2O$ ), 7.13–7.24 (m, 10H,  $2C_6H_5$ ) ppm.

**Preparation of  $[(\mu-PhS)Fe_2(CO)_6]_2[\mu-SCH_2(CH_2OCH_2)_3-CH_2S-\mu]$  (6b).** The same procedure was followed as for **6a**, but  $4 \cdot [Et_3NH]_2$  ( $Z = CH_2(CH_2OCH_2)_3CH_2$ ) was used. From the main red band, 0.410 g (41%) of **6b** was obtained as a red oil. Anal. Calcd for  $C_{32}H_{26}Fe_4O_{15}S_4$ : C, 38.35; H, 2.61. Found: C, 38.22; H, 2.55. IR (KBr disk):  $\nu_{C=O}$  2071 (s), 2033 (vs), 1993 (vs);  $\nu_{C-O-C}$  1116 (m)  $cm^{-1}$ .  $^1H$  NMR (200 MHz,  $CDCl_3$ ): 2.56 (s, 4H,  $2CH_2S$ ), 3.58 (s, 12H,  $6CH_2O$ ), 7.24 (s, 10H,  $2C_6H_5$ ) ppm.

**Preparation of  $[Fe_2(CO)_6]_2[\mu-S-S-\mu][\mu-SCH_2(CH_2OCH_2)_2-CH_2S-\mu]$  (7a).** To the above-prepared solution of  $4 \cdot [Et_3NH]_2$  ( $Z = CH_2(CH_2OCH_2)_2CH_2$ ) was added 0.16 mL (2.0 mmol) of  $S_2Cl_2$ , and the mixture was stirred at room temperature for 4 h. Solvent was removed under reduced pressure. The residue was subjected to TLC separation using acetone/petroleum ether (1/10 v/v) as eluent. From the main red band, 0.103 (13% yield) of **7a** was obtained as a red solid, mp 155 °C dec. Anal. Calcd for  $C_{18}H_{12}Fe_4O_{14}S_4$ : C, 26.89; H, 1.50. Found: C, 26.85; H, 1.45. IR (KBr disk):  $\nu_{C=O}$  2080 (s), 2067 (s), 2045 (vs), 2022 (vs), 1998 (vs), 1980 (vs);  $\nu_{C-O-C}$  1127 (m)  $cm^{-1}$ .  $^1H$  NMR (200 MHz,  $CDCl_3$ ): 2.24–2.30, 2.70–2.75 (m, m, 4H,  $2CH_2S$ ), 3.27–3.78 (m, 8H,  $4CH_2O$ ) ppm.

**Preparation of  $[Fe_2(CO)_6]_2[\mu-S-S-\mu][\mu-SCH_2(CH_2OCH_2)_3-CH_2S-\mu]$  (7b).** The same procedure was followed as for **7a**, but  $4 \cdot [Et_3NH]_2$  ( $Z = CH_2(CH_2OCH_2)_3CH_2$ ) was employed. From the main red band, 0.149 g (18% yield) of **7b** was obtained as a red solid, mp 148 °C dec. Anal. Calcd for  $C_{20}H_{16}Fe_4O_{15}S_4$ : C, 28.33; H, 1.90. Found: C, 28.20; H, 1.91. IR (KBr disk):  $\nu_{C=O}$  2081 (s), 2069 (s), 2046 (vs), 2022 (vs), 1999 (vs), 1980 (vs);  $\nu_{C-O-C}$  1128 (m)  $cm^{-1}$ .  $^1H$  NMR (200 MHz,  $CDCl_3$ ): 2.13–2.20, 2.70–2.79 (m, m, 4H,  $2CH_2S$ ), 3.26–3.83 (m, 12H,  $6CH_2O$ ) ppm.

**Preparation of  $[Fe_2(CO)_6]_2[\mu-SCH_2(CH_2OCH_2)_2CH_2S-\mu]_2$  (8a).** After the above-prepared solution of  $4 \cdot [Et_3NH]_2$  ( $Z = CH_2(CH_2OCH_2)_2CH_2$ ) was cooled to  $-10$  °C, 0.252 g (1.0 mmol) of  $ClCH_2(CH_2OCH_2)_2CH_2S-Cl$  was added. The mixture was stirred at room temperature for 12 h. Solvent was removed under reduced pressure. The residue was subjected to TLC separation using acetone/petroleum ether (1/3 v/v) as eluent. From the main red band, 0.132 g (14%) of **8a** was obtained as a red solid, mp 146–148 °C. Anal. Calcd for  $C_{24}H_{24}Fe_4O_{16}S_4$ : C, 31.33; H, 2.63. Found: C, 31.19; H, 2.89. IR (KBr disk):  $\nu_{C=O}$  2071 (s), 2036 (vs), 1995 (vs), 1966 (vs);  $\nu_{C-O-C}$  1119 (s)  $cm^{-1}$ .  $^1H$  NMR (200 MHz,  $CDCl_3$ ): 2.27–2.71 (m, 8H,  $4CH_2S$ ), 3.44–3.96 (m, 16H,  $8CH_2O$ ) ppm.

**Preparation of  $[Fe_2(CO)_6]_2[\mu-SCH_2(CH_2OCH_2)_3CH_2S-\mu]_2$  (8b).** The same procedure was followed as for **8a**, but  $4 \cdot [Et_3NH]_2$  ( $Z = CH_2(CH_2OCH_2)_3CH_2$ ) was employed. From the main red band, 0.148 g (15%) of **8b** was obtained as a red solid, mp 148 °C dec. Anal. Calcd for  $C_{28}H_{32}Fe_4O_{18}S_4$ : C, 33.36; H, 3.20. Found: C, 33.30; H, 3.15. IR (KBr disk):  $\nu_{C=O}$  2068 (s), 2031 (vs), 1994 (vs), 1975 (s);  $\nu_{C-O-C}$  1127 (s)  $cm^{-1}$ .  $^1H$  NMR

(200 MHz,  $CDCl_3$ ): 2.32–2.68 (m, 8H,  $4CH_2S$ ), 3.38–3.87 (m, 24H,  $12CH_2O$ ) ppm.

**Preparation of  $[(\mu-PhNHC=S)Fe_2(CO)_6]_2[\mu-SCH_2CH_2-OCH_2CH_2S-\mu]$  (9a).** To the above-prepared solution of  $4 \cdot [Et_3NH]_2$  ( $Z = CH_2CH_2OCH_2CH_2$ ) was added 0.24 mL (2.0 mmol) of  $PhN=C=S$ , and the mixture was stirred at room temperature for 12 h. Solvent was removed under reduced pressure. The residue was subjected to TLC separation. Acetone/petroleum ether (1/4 v/v) eluted the first main red band, which gave 0.387 g (40%) of **9a** as an orange solid, mp 68–70 °C. Anal. Calcd for  $C_{30}H_{20}Fe_4N_2O_{13}S_4$ : C, 37.22; H, 2.08; N, 2.89. Found: C, 37.21; H, 2.11; N, 2.85. IR (KBr disk):  $\nu_{C=O}$  2065 (vs), 2024 (vs), 1989 (vs);  $\nu_{N-H}$  3380 (m);  $\nu_{C-O-C}$  1107 (m);  $\nu_{C-S}$  943 (w)  $cm^{-1}$ .  $^1H$  NMR (200 MHz,  $CDCl_3$ ): 2.86–2.94 (m, 4H,  $2CH_2S$ ), 3.93 (t,  $J = 6.4$  Hz, 4H,  $2CH_2O$ ), 7.24–7.31 (m, 10H,  $2C_6H_5$ ), 8.73 (s, 2H, 2NH) ppm.

**Preparation of  $[(\mu-PhNHC=S)Fe_2(CO)_6]_2[\mu-SCH_2-(CH_2OCH_2)_2CH_2S-\mu]$  (9b).** The same procedure was followed as for **9a**, but  $4 \cdot [Et_3NH]_2$  ( $Z = CH_2(CH_2OCH_2)_2CH_2$ ) was utilized. The residue was subjected to TLC separation using acetone/petroleum ether (1/10 v/v) as eluent. From the main red band, 0.705 g (70%) of **9b** was obtained as an orange solid, mp 68–71 °C. Anal. Calcd for  $C_{32}H_{24}Fe_4N_2O_{14}S_4$ : C, 37.97; H, 2.39; N, 2.77. Found: C, 37.85; H, 2.48; N, 3.04. IR (KBr disk):  $\nu_{C=O}$  2064 (vs), 2024 (vs), 1989 (vs);  $\nu_{N-H}$  3379 (m);  $\nu_{C-O-C}$  1113 (m);  $\nu_{C-S}$  940 (w)  $cm^{-1}$ .  $^1H$  NMR (200 MHz,  $CDCl_3$ ): 2.80 (s, 4H,  $2CH_2S$ ), 3.63–3.85 (m, 8H,  $4CH_2O$ ), 7.26 (s, 10H,  $2C_6H_5$ ), 8.69 (s, 2H, 2NH) ppm.

**Preparation of  $[(\mu-PhNHC=S)Fe_2(CO)_6]_2[\mu-SCH_2-(CH_2OCH_2)_3CH_2S-\mu]$  (9c).** The same procedure was followed as for **9a**, but  $4 \cdot [Et_3NH]_2$  ( $Z = CH_2(CH_2OCH_2)_3CH_2$ ) was employed. From the main red band, 0.698 g (66%) of **9c** was obtained as an orange solid, mp 55–57 °C. Anal. Calcd for  $C_{34}H_{28}Fe_4N_2O_{15}S_4$ : C, 38.66; H, 2.67; N, 2.65. Found: C, 38.74; H, 2.78; N, 3.04. IR (KBr disk):  $\nu_{C=O}$  2064 (vs), 2024 (vs), 1988 (vs);  $\nu_{N-H}$  3379 (m);  $\nu_{C-O-C}$  1111 (m);  $\nu_{C-S}$  941 (w)  $cm^{-1}$ .  $^1H$  NMR (200 MHz,  $CDCl_3$ ): 2.84 (s, 4H,  $2CH_2S$ ), 3.65–3.95 (m, 12H,  $6CH_2O$ ), 7.30 (s, 10H,  $2C_6H_5$ ), 8.74 (s, 2H, 2NH) ppm.

**Preparation of  $[Fe_2(CO)_6]_2[\mu-S=CNH(CH_2)_4NHC=S-\mu]-(\mu-SCH_2)_4S-\mu]$  (10a).** To the above-prepared solution of  $4 \cdot [Et_3NH]_2$  ( $Z = (CH_2)_4$ ) was added 0.172 g (1.0 mmol) of  $SCN(CH_2)_4NCS$ , and the mixture was stirred at room temperature for 12 h. Solvent was removed under reduced pressure. The residue was subjected to TLC separation using acetone/petroleum ether (1/1 v/v) as eluent. From the main red band, 0.146 g (17%) of **10a** was obtained as a red oil. Anal. Calcd for  $C_{22}H_{18}Fe_4N_2O_{12}S_4$ : C, 30.94; H, 2.12; N, 3.28. Found: C, 31.11; H, 2.19; N, 3.39. IR (KBr disk):  $\nu_{C=O}$  2069 (v), 2025 (vs), 1963 (vs);  $\nu_{C-S}$  1026 (m)  $cm^{-1}$ .  $^1H$  NMR (200 MHz,  $CDCl_3$ ): 1.35–2.10 (m, 8H,  $2CH_2CH_2CH_2CH_2$ ), 2.40–2.65 (m, 4H,  $2CH_2S$ ), 2.80–2.95 (m, 4H,  $2CH_2N$ ), 6.56 (s, 2H, 2HN) ppm.

**Preparation of  $[Fe_2(CO)_6]_2[\mu-S=CNH(CH_2)_4NHC=S-\mu]-(\mu-SCH_2(CH_2OCH_2)_2CH_2S-\mu)$  (10b).** The same procedure was followed as for **10a**, but  $4 \cdot [Et_3NH]_2$  ( $Z = CH_2(CH_2OCH_2)_2CH_2$ ) was utilized. From the main red band, 0.118 g (13%) of **10b** was obtained as a red oil. Anal. Calcd for  $C_{24}H_{22}Fe_4N_2O_{12}S_4$ : C, 31.54; H, 2.43; N, 3.06. Found: C, 31.70; H, 2.22; N, 3.25. IR (KBr disk):  $\nu_{C=O}$  2063 (s), 2017 (vs), 1944 (vs);  $\nu_{C-O-C}$  1093 (m);  $\nu_{C-S}$  1025 (m)  $cm^{-1}$ .  $^1H$  NMR (200 MHz,  $CDCl_3$ ): 1.35–2.12 (m, 4H,  $CH_2CH_2CH_2CH_2$ ), 2.24–2.80 (m, 4H,  $2CH_2S$ ), 2.75–3.18 (m, 4H,  $2CH_2N$ ), 3.71 (br.s, 8H,  $4CH_2O$ ), 6.62 (s, 2H, 2HN) ppm.

**Preparation of  $[(\mu-\sigma,\pi-PhCH=CPh)Fe_2(CO)_6]_2[\mu-SCH_2-(CH_2OCH_2)_2CH_2S-\mu]$  (11a).** To the above-prepared solution of  $4 \cdot [Et_3NH]_2$  ( $Z = CH_2(CH_2OCH_2)_2CH_2$ ) was added 0.356 g (2.0 mmol) of  $PhC\equiv CPh$ . The mixture was refluxed for 45 min. Solvent was removed under reduced pressure. The residue was subjected to TLC separation using acetone/petroleum ether (1/10 v/v) as eluent. From the main red band, 0.200 g (18%) of **11a** was obtained as a red solid, mp 67–69 °C. Anal. Calcd for  $C_{46}H_{32}Fe_4O_{14}S_2$ : C, 50.40; H, 2.94. Found: C, 50.08; H, 3.13.



Table 5. Crystal Data and Structural Refinement Details for 5a, 7a, 8a, and 12a

	5a	7a	8a	12a
mol formula	C <sub>22</sub> H <sub>18</sub> Fe <sub>4</sub> O <sub>12</sub> S <sub>2</sub>	C <sub>18</sub> H <sub>12</sub> Fe <sub>4</sub> O <sub>14</sub> S <sub>4</sub>	C <sub>24</sub> H <sub>24</sub> Fe <sub>4</sub> O <sub>16</sub> S <sub>4</sub>	C <sub>32</sub> H <sub>22</sub> Fe <sub>4</sub> O <sub>12</sub> S <sub>2</sub>
mol wt	761.8	803.92	920.07	886.02
temp/K	293(2)	293(2)	293(2)	293(2)
cryst syst	triclinic	triclinic	triclinic	triclinic
space group	<i>P</i> $\bar{1}$	<i>P</i> $\bar{1}$	<i>P</i> $\bar{1}$	<i>P</i> $\bar{1}$
<i>a</i> /Å	7.949(4)	9.301(6)	8.224(3)	7.689(2)
<i>b</i> /Å	8.814(4)	11.760(8)	9.766(3)	13.441(4)
<i>c</i> /Å	11.157(5)	14.532(10)	11.153(4)	19.125(6)
$\alpha$ /deg	98.568(8)	103.889(11)	88.962(6)	75.116(5)
$\beta$ /deg	98.011(8)	97.842(11)	81.064(6)	87.337(5)
$\gamma$ /deg	110.770(8)	104.773(10)	88.230(6)	74.286(6)
<i>V</i> /Å <sup>3</sup>	706.9(6)	1458.5(17)	884.4(5)	1838.3(9)
<i>Z</i>	1	2	1	2
<i>D</i> <sub>c</sub> /g cm <sup>-3</sup>	1.790	1.831	1.728	1.601
abs coeff/mm <sup>-1</sup>	2.218	2.298	1.911	1.719
<i>F</i> (000)	382	800	464	892
limiting indices	-7 ≤ <i>h</i> ≤ 9 -10 ≤ <i>k</i> ≤ 11 -10 ≤ <i>l</i> ≤ 13	-11 ≤ <i>h</i> ≤ 10 -9 ≤ <i>k</i> ≤ 13 -17 ≤ <i>l</i> ≤ 10	-10 ≤ <i>h</i> ≤ 10 -12 ≤ <i>k</i> ≤ 6 -13 ≤ <i>l</i> ≤ 13	-9 ≤ <i>h</i> ≤ 8 -11 ≤ <i>k</i> ≤ 15 -18 ≤ <i>l</i> ≤ 22
scan type	$\omega$ -2 $\theta$	$\omega$ -2 $\theta$	$\omega$ -2 $\theta$	$\omega$ -2 $\theta$
no. of rflns	3350	7291	5103	7198
no. of indep rflns	2643	5041	3574	6370
<i>R</i> <sub>int</sub>	0.0243	0.0204	0.0331	0.0324
2 $\theta$ <sub>max</sub> /deg	52.88	50.00	52.86	50.06
no. of data/restraints/params	2643/0/181	5041/304/399	3574/0/217	6370/0/451
<i>R</i>	0.0392	0.0434	0.0504	0.0516
<i>R</i> <sub>w</sub>	0.0706	0.1437	0.1161	0.1025
goodness of fit	0.931	1.087	1.065	1.014
largest diff peak and hole/e Å <sup>-3</sup>	0.501 and -0.323	0.816 and -0.783	0.515 and -0.411	0.381 and -0.320

IR (KBr disk):  $\nu_{C=O}$  2066 (s), 2036 (vs), 1990 (vs);  $\nu_{C-O-C}$  1125 (m);  $\nu_{C=C}$  1001 (w) cm<sup>-1</sup>. <sup>1</sup>H NMR (200 MHz, CDCl<sub>3</sub>): 2.63 (s, 4H, 2CH<sub>2</sub>S), 3.66–3.77 (m, 10H, 4CH<sub>2</sub>O, 2PhCH), 6.69–7.24 (m, 20H, 4C<sub>6</sub>H<sub>5</sub>) ppm.

**Preparation of [( $\mu$ - $\sigma$ , $\pi$ -PhCH=CPh)Fe<sub>2</sub>(CO)<sub>6</sub>]<sub>2</sub>[ $\mu$ -SCH<sub>2</sub>-(CH<sub>2</sub>OCH<sub>2</sub>)<sub>3</sub>CH<sub>2</sub>S- $\mu$ ] (11b).** The same procedure was followed as for 11a, but 4·[Et<sub>3</sub>NH]<sub>2</sub> (Z = CH<sub>2</sub>(CH<sub>2</sub>OCH<sub>2</sub>)<sub>3</sub>CH<sub>2</sub>) was used. From the main red band, 0.182 g (16%) of 11b was obtained as a red solid, mp 54–55 °C. Anal. Calcd for C<sub>48</sub>H<sub>36</sub>Fe<sub>4</sub>O<sub>15</sub>S<sub>2</sub>: C, 50.56; H, 3.18. Found: C, 50.54; H, 3.38. IR (KBr disk):  $\nu_{C=O}$  2064 (s), 2033 (vs), 1990 (vs);  $\nu_{C-O-C}$  1116 (m);  $\nu_{C=C}$  992 (w) cm<sup>-1</sup>. <sup>1</sup>H NMR (200 MHz, CDCl<sub>3</sub>): 2.62 (s, 4H, 2CH<sub>2</sub>S), 3.64–3.75 (m, 14H, 6CH<sub>2</sub>O, 2PhCH), 6.69–7.24 (m, 20H, 4C<sub>6</sub>H<sub>5</sub>) ppm.

**Preparation of [( $\mu$ - $\sigma$ , $\pi$ -PhCH=CH)Fe<sub>2</sub>(CO)<sub>6</sub>]<sub>2</sub>[ $\mu$ -S(CH<sub>2</sub>)<sub>4</sub>S- $\mu$ ] (12a).** To the above-prepared solution of 4·[Et<sub>3</sub>NH]<sub>2</sub> (Z = (CH<sub>2</sub>)<sub>4</sub>) was added 0.408 g (4.0 mmol) of PhC≡CH. The mixture was refluxed for 1 h and stirred at room temperature for 3 h. Solvent was removed under reduced pressure. The residue was subjected to TLC separation using CH<sub>2</sub>Cl<sub>2</sub>/petroleum ether (1/1 v/v) as eluent. From the main red band, 0.450 g (51%) of 12a was obtained as a red solid, mp 167 °C dec. Anal. Calcd for C<sub>32</sub>H<sub>22</sub>Fe<sub>4</sub>O<sub>12</sub>S<sub>2</sub>: C, 43.38; H, 2.50. Found: C, 43.42; H, 2.49. IR (KBr disk):  $\nu_{C=O}$  2068 (vs), 2036 (vs), 1985 (vs);  $\nu_{C=C}$  1597 (w) cm<sup>-1</sup>. <sup>1</sup>H NMR (200 MHz, CDCl<sub>3</sub>): 1.82 (s, 4H, SCH<sub>2</sub>CH<sub>2</sub>CH<sub>2</sub>CH<sub>2</sub>S), 2.38 (s, 4H, 2CH<sub>2</sub>S), 4.35 (d, *J* = 13.8 Hz, 2H, 2 endo-PhCH), 7.27 (s, 10H, 2C<sub>6</sub>H<sub>5</sub>), 8.46 (d, 2H, *J* = 13.8 Hz, 2 exo-FeCH) ppm.

**Preparation of [( $\mu$ - $\sigma$ , $\pi$ -PhCH=CH)Fe<sub>2</sub>(CO)<sub>6</sub>]<sub>2</sub>[ $\mu$ -SCH<sub>2</sub>-(CH<sub>2</sub>OCH<sub>2</sub>)<sub>2</sub>CH<sub>2</sub>S- $\mu$ ] (12b).** The same procedure was followed as for 12a, but 4·[Et<sub>3</sub>NH]<sub>2</sub> (Z = CH<sub>2</sub>(CH<sub>2</sub>OCH<sub>2</sub>)<sub>2</sub>CH<sub>2</sub>) was used. From the main red band, 0.374 g (40%) of 12b was obtained as a red solid, mp 121 °C dec. Anal. Calcd for C<sub>34</sub>H<sub>26</sub>Fe<sub>4</sub>O<sub>14</sub>S<sub>2</sub>: C, 43.16; H, 2.77. Found: C, 42.97; H, 3.01. IR (KBr disk):  $\nu_{C=O}$  2069 (vs), 2038 (vs), 1988 (vs);  $\nu_{C=C}$  1597 (w);  $\nu_{C-O-C}$  1126 (s) cm<sup>-1</sup>. <sup>1</sup>H NMR (200 MHz, CDCl<sub>3</sub>): 2.57 (t, *J* = 6.0 Hz, 4H, 2CH<sub>2</sub>S), 3.70 (s, 4H, 4CH<sub>2</sub>O), 4.33 (d, *J* = 13.8 Hz, 2H, 2 endo-PhCH), 7.26 (s, 10H, 2C<sub>6</sub>H<sub>5</sub>), 8.45 (d, *J* = 13.8 Hz, 2H, 2 exo-FeCH) ppm.

**Preparation of [( $\mu$ - $\sigma$ , $\pi$ -PhCH=CH)Fe<sub>2</sub>(CO)<sub>6</sub>]<sub>2</sub>[ $\mu$ -SCH<sub>2</sub>-(CH<sub>2</sub>OCH<sub>2</sub>)<sub>3</sub>CH<sub>2</sub>S- $\mu$ ] (12c).** The same procedure was followed as for 12a, but 4·[Et<sub>3</sub>NH]<sub>2</sub> (Z = CH<sub>2</sub>(CH<sub>2</sub>OCH<sub>2</sub>)<sub>3</sub>CH<sub>2</sub>) was utilized. From the main red band, 0.444 g (45%) of 12c was obtained as a red solid, mp 135 °C dec. Anal. Calcd for C<sub>36</sub>H<sub>30</sub>-Fe<sub>4</sub>O<sub>15</sub>S<sub>2</sub>: C, 43.67; H, 3.05. Found: C, 43.60; H, 3.06. IR (KBr disk):  $\nu_{C=O}$  2068 (vs), 2036 (vs), 1988 (vs);  $\nu_{C=C}$  1596 (w);  $\nu_{C-O-C}$  1124 (s) cm<sup>-1</sup>. <sup>1</sup>H NMR (200 MHz, CDCl<sub>3</sub>): 2.57 (s, 4H, 2CH<sub>2</sub>S), 3.69 (s, 12H, 6CH<sub>2</sub>O), 4.32 (d, *J* = 13.8 Hz, 2H, 2 endo-PhCH), 7.24 (s, 10H, 2C<sub>6</sub>H<sub>5</sub>), 8.44 (d, *J* = 13.8 Hz, 2H, 2 exo-FeCH) ppm.

**X-ray Structure Determinations of 5a, 7a, 8a, and 12a.** Single crystals of 5a, 7a, 8a, and 12a suitable for X-ray diffraction analyses were grown by slow evaporation of their CH<sub>2</sub>Cl<sub>2</sub>/petroleum ether solutions at -20 °C for 7a and at about 4 °C for 5a, 8a, and 12a. Each crystal was mounted on a Bruker SMART 1000 automated diffractometer with a graphite monochromator with Mo K $\alpha$  radiation ( $\lambda$  = 0.710 73 Å). The structures were solved by direct methods and expanded by Fourier techniques. The final refinements were accomplished by the full-matrix least-squares method with anisotropic thermal parameters for non-hydrogen atoms. The calculations were performed using the SHELXTL-97 program. Details of the crystal data, data collections, and structure refinements are summarized in Table 5.

**Acknowledgment.** We are grateful to the National Natural Science Foundation of China and the Research Fund for the Doctoral Program of Higher Education of China for financial support.

**Supporting Information Available:** All crystal data, atomic coordinates and thermal parameters and bond lengths and angles for 5a, 7a, 8a, and 12a as CIF files. This material is available free of charge via the Internet at <http://pubs.acs.org>.

OM034208F